Neuro-Oncology
23(10), 1693–1708, 2021 | doi:10.1093/neuonc/noab126 | Advance Access date 27 May 2021

Spliceosome-regulated RSRP1-dependent NF-κB activation promotes the glioblastoma mesenchymal phenotype

Yaomin Li[†], Xiran Wang[†], Songtao Qi[†], Lei Gao, Guanglong Huang, Zhonglu Ren, Kaishu Li, Yuping Peng, Guozhong Yi, Jinglin Guo, Runwei Yang, Hai Wang, Xian Zhang, and Yawei Liu

Department of Neurosurgery, Nanfang Hospital, Southern Medical University, Guangzhou, Guangdong, China (Y.L., X.W., S.Q., L.G., G.H., K.L., Y.P., G.Y., J.G., R.Y., H.W., X.Z., Y.L.); Laboratory for Precision Neurosurgery, Nanfang Hospital, Southern Medical University, Guangzhou, Guangdong, China (Y.L., X.W., S.Q., L.G., G.H., K.L., Y.P., G.Y., J.G., R.Y., H.W., X.Z., Y.L.); College of Medical Information Engineering, Guangdong Pharmaceutical University, Guangzhou, Guangdong, China (Z.R.)

Corresponding Authors: Yawei Liu, MD, PhD, Guangzhou Dadao Bei Street 1838#, Guangzhou 510515, China (liuyawei@smu.edu.cn); Xian Zhang, MD, PhD, Guangzhou Dadao Bei Street 1838#, Guangzhou 510515, China (zxa@smu.edu.cn).

[†]These authors contributed equally to this work.

Abstract

Background. The glioblastoma (GBM) mesenchymal (MES) phenotype, induced by NF-κB activation, is characterized by aggressive tumor progression and poor clinical outcomes. Our previous analysis indicated that MES GBM has a unique alternative splicing (AS) pattern; however, the underlying mechanism remains obscure. We aimed to reveal how splicing regulation contributes to MES phenotype promotion in GBM.

Methods. We screened novel candidate splicing factors that participate in NF-κB activation and MES phenotype promotion in GBM. In vitro and in vivo assays were used to explore the function of RSRP1 in MES GBM.

Results. Here, we identified that arginine/serine-rich protein 1 (RSRP1) promotes the MES phenotype by facilitating GBM cell invasion and apoptosis resistance. Proteomic, transcriptomic, and functional analyses confirmed that RSRP1 regulates AS in MES GBM through mediating spliceosome assembly. One RSRP1-regulated AS event resulted in skipping PARP6 exon 18 to form truncated, oncogenic PARP6-s. This isoform was unable to effectively suppress NF-κB. Cotreatment of cultured GBM cells and GBM tumor-bearing mice with spliceosome and NF-κB inhibitors exerted a synergistic effect on MES GBM growth.

Conclusion. We identified a novel mechanism through which RSRP1-dependent splicing promotes the GBM MES phenotype. Targeting AS via RSRP1-related spliceosomal factors might constitute a promising treatment for GBM.

Key Points

1. RSRP1 is a novel factor contributing to spliceosome assembly via serine phosphorylation.
2. RSRP1-regulated PARP6 isoform switching activates NF-κB in GBM.
3. Our data support clinical trials of the spliceosome and NF-κB inhibitors in GBM.

Glioblastoma (GBM) is the most malignant and common primary brain tumor[1] and is a prototypal example of heterogeneous cancer.[2] Intratumor heterogeneity poses a challenge for diagnosis and may underlie the observed inefficiencies of conventional and single-target GBM treatments.[2–4] To better understand GBM heterogeneity, The Cancer Genome Atlas (TCGA) consortium proposed a molecular classification system that comprises four subtypes:

Importance of the Study

The glioblastoma (GBM) mesenchymal (MES) phenotype is characterized by aggressive tumor progression and poor clinical outcomes. Identification of regulatory mechanisms that promote the MES phenotype is critical for developing GBM therapy. Our previous study supports that the MES phenotype of GBM exhibits a unique alternative splicing (AS) pattern, which indicates that splicing progression participates in MES promotion. Here, we identified a novel spliceosomal factor, RSRP1, that contributes to spliceosome assembly in GBM cells. While previous studies have demonstrated that the role of PARPs in NF-κB activation is isoform specific, our data show that RSRP1 regulates the isoform switching of PARP6 and further activates NF-κB, thereby promoting the GBM MES phenotype. Finally, preclinical experiments support that targeting the spliceosome-regulated NF-κB axis might be a therapeutic strategy for GBM patients.

classical (CL), mesenchymal (MES), neural (NE), and proneural (PN).[5] Glioma stem cells (GSCs) contribute to tumor initiation and treatment resistance; they can be derived from GBM tissues and classified as the CL, MES, or PN subtype based on their expression markers. MES identity is a hallmark of GBM aggressiveness and a poor prognosis.[6] MES phenotypic transition has been identified in GBM in response to treatments and is now termed the PN to MES transition (PMT).[7] Therefore, targeting MES GSCs might be a prospective therapy for GBM.

Nuclear factor-kappa B (NF-κB) activation has an important role in the MES transition of GSCs and is associated with poor outcomes in GBM.[6] Consequently, MES GSCs might be targeted by suppressing the NF-κB pathway.[8] Inhibitors of NF-κB have been developed and are used in clinical practice as treatments for diabetes, lymphoma, and breast cancer.[9–11] Preclinical studies showed promising results when targeting the NF-κB pathway for the treatment of GBM; however, the clinical success has been limited; for example, a phase 1/2 trial using sulfasalazine showed a lack of response,[12] which might have resulted from GBM heterogeneity. Recent studies have focused on identifying novel targets in GBM and testing combinatory treatments to enhance the antitumor effects while ensuring drug safety.[13,14] Revealing the mechanism underlying NF-κB activation in MES GBM might provide a theoretical foundation for novel treatments.

Differences in alternative splicing (AS) are another form of intratumor heterogeneity in GBM, and recent studies, including ours, have shown that GBM phenotypes have unique AS patterns.[15] These findings indicate the crucial role of splicing regulation in GBM.

Splicing progression is regulated by spliceosomes, which are complex molecular machines composed of several spliceosomal factors, some of which serve as therapeutic targets in various cancers.[16] Among these proteins, SR-related proteins are defined as those that contain an arginine/serine (RS) domain, which is extensively phosphorylated and promotes protein-protein interactions involved in spliceosome assembly.[17]

Here, we sought to identify and characterize novel SR-related proteins in spliceosomes involved in promoting the MES phenotype in GBM GSCs. We found that arginine/serine-rich protein 1 (RSRP1), a novel SR-related protein with an RS domain, is significantly upregulated in MES GSCs compared with PN GSCs, but its function has been unclear thus far. This study presents evidence that RSRP1 plays an important role in promoting the MES phenotype of GBM through splicing regulation.

Methods

Data Acquisition

The data supporting the findings of this study are available within the article and its Supplementary Materials.

Patient-Derived Glioma Specimens and Cell Lines

All glioma samples were obtained after surgical resection from patients admitted to the Department of Neurosurgery, Nanfang Hospital (NFH), Southern Medical University, China, and the corresponding clinical data were collected. The glioma specimens were obtained for pathological examination and cell isolation. GSCs isolated from specimens were verified by immunofluorescence (IF) (Supplementary Figure S1C) and xenograft assays, as previously described.[18] Established GBM cell lines (LN229, U87MG, T98G, and A172) were purchased from the American Type Culture Collection (ATCC, USA). The cell lines were cultured as previously described.[18]

Ethics Approval and Consent to Participate

The experimental protocol was established according to the ethical guidelines of the Helsinki Declaration and was approved by the Ethics Committee of Southern Medical University, China. Written informed consent was obtained from individual participants or their guardians. All animal experiments were performed following approval of the Institutional Animal Care and Use Committee of Southern Medical University, China.

Immunohistochemistry

Immunohistochemistry (IHC) assays were performed with glioma specimens and xenografts, which were scored to determine the relative expression levels based on standard procedures listed in the Supplementary Materials.

Protein Extraction, Western Blotting, Coimmunoprecipitation, and Mass Spectrometry

Protein extraction, western blotting (WB), coimmunoprecipitation (Co-IP), mass spectrometry, and further bioinformatic analysis were performed as previously described.[19] Protein expression was then quantified with ImageJ software (version 1.8.0) (https://imagej.nih.gov/ij/).

IF Assays

IF assays were performed with the indicated antibodies as previously described.[18] Images were captured under a Carl-Zeiss LSM 880 confocal microscope equipped with ZEN 2 software (version 4.0) for image acquisition and analysis.

RNA Isolation and Reverse Transcription-Polymerase Chain Reaction

Total RNA was isolated as previously described.[18] Reverse transcription-polymerase chain reaction (RT-PCR) was performed to detect RSRP1-regulated AS. The following primers were synthesized by Invitrogen: poly(ADP-ribose) polymerase 6 (PARP6) (forward: 5′-TGGAAATCAAGAAACAGATGGA-3′, reverse: 5′-TGGAGATGGGGCTCAGGTA-3′); RPS25 (forward: 5′-CTGCGGTGTCTGCTGCTA-3′, reverse: 5′-GCTTGTCCCGAACTTTGC-3′); TNFRSF12A (forward: 5′-TCTGGCTGGCGTTGCTGC-3′, reverse: 5′-GCGTGAGGCTCCCTTTCTGTTCT-3′); EXOC7 (forward: 5′-TACTCCCCTGCTATCCCCAA-3′, reverse: 5′-ATGTAGGCATCGGTCTCCAC-3′); and KIF13B (forward: 5′-AGCAGGATGTATCCCAAACCACA-3′, reverse: 5′-AGTACCCGCTAGAGGCTTCACTCA-3′).

Establishment of RSRP1-Knockout Cells

The CRISPR/Cas9 system was used to establish RSRP1-knockout (KO) cells (LN229 and NFH-GSC1) according to the manufacturer's instructions, as described within the Supplementary Materials.

Antibodies and Reagents

The antibodies and reagents of this study are available in the Supplementary Materials.

Cell Counting Kit-8 and Transwell Migration Assays

Cell counting kit-8 (CCK-8) and Transwell migration assays were performed as previously described.[18]

Flow Cytometry

Flow cytometry was performed to analyze the cell cycle and cell apoptosis. The Cell Cycle Detection Kit (KGA511, Keygen) and Annexin V-FITC/PI Apoptosis Detection Kit (S0185, Keygen) were used for cell cycle and cell apoptosis analyses, respectively. BD FACSDiva software (version 8.0.1) was used for analysis.

RNA-seq and Data Analysis

The LN229 and NFH-GSC1 cell lines were stably transfected with control or RSRP1-WT lentiviruses, as described above. Total RNA isolation, library construction, and sequencing were conducted using an Illumina HiSeq 2000 system, following the standard instructions. AS analysis was conducted using rMATs software (http://rnaseq-mats.sourceforge.net/index.html).

In Vivo Assays

The subcutaneous and intracranial xenograft experimental procedures are available in the Supplementary Materials.

Statistical Analyses

Statistical analyses were performed using SPSS software (version 23.0, IBM). Student's *t* tests, Mann–Whitney *U* tests, one-way ANOVA, Pearson correlation analyses, Kaplan–Meier analyses, log-rank tests, Cox's proportional hazards regression model, and χ^2 tests were used to analyze the corresponding data, as detailed in the figure legends.

Results

RSRP1 Is a Marker of MES GBM

To investigate the essential factors that participate in GBM MES phenotype maintenance through splicing regulation, we analyzed the upregulated genes in spliceosome-enriched samples in the TCGA database. The spliceosome expression score of each sample was calculated according to the mean value of log2(TPM+1) for each spliceosome gene. We regarded the median spliceosome expression score (Supplementary Table S1) as the threshold for defining a sample as either "spliceosome enriched" or "not spliceosome enriched." We also analyzed the genes upregulated in MES GBM samples compared to PN GBM samples based on TCGA classification data.[20] We identified 636 genes that were mutually upregulated in the spliceosome-enriched and MES samples (Figure 1A). The NF-κB pathway plays an important role in MES phenotype determination in GBM by regulating a defined set of genes, and we used 16 of these genes to construct an NF-κB activation signature (Supplementary Table S1).[6,21] Then, we used these signature genes to identify samples with activated NF-κB and defined the upregulated genes in these samples. Interestingly, we found that the vast majority of the mutually upregulated genes (98.6%, 627/636) in spliceosome-enriched and MES samples were also upregulated in the activated NF-κB group (Supplementary Table S2) (Figure 1A), indicating that spliceosomes might promote the MES phenotype in GSCs via the NF-κB pathway.

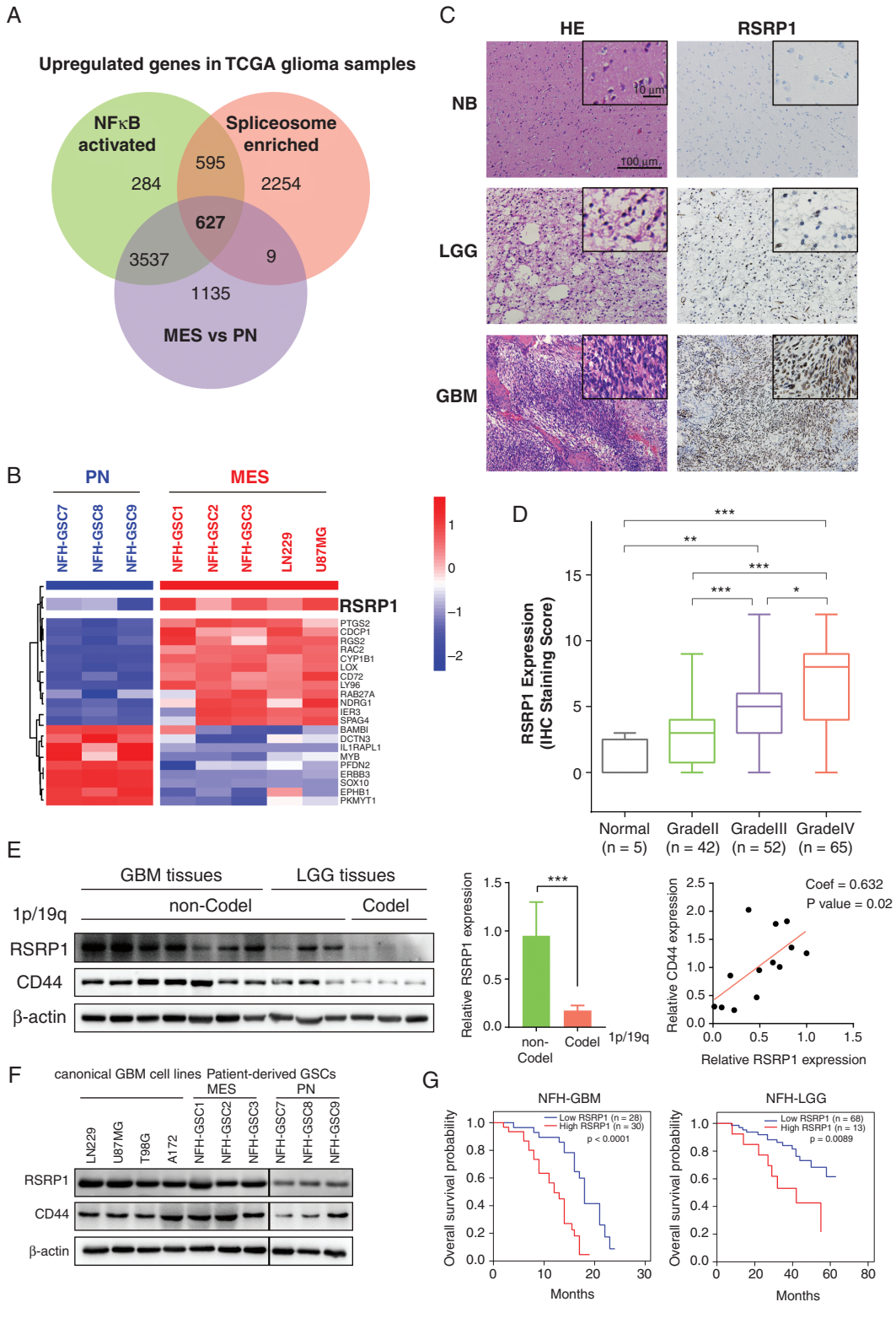

Fig. 1 Increased RSRP1 expression is related to a more malignant glioblastoma (GBM) phenotype. (A) Venn diagram showing the upregulated genes in GBM samples from The Cancer Genome Atlas (TCGA) database. Green circle: upregulated genes in samples with activated NF-κB. Red circle: upregulated genes in spliceosome-enriched samples. Purple circle: genes upregulated in MES GBM samples compared to PN GBM samples. (B) Heatmap showing differentially expressed subtype signatures and expression levels of RSRP1 in 3 PN glioblastoma cell lines versus 5 MES GBM cell lines. (C) Representative hematoxylin and eosin (HE) staining and immunohistochemistry (IHC) staining for RSRP1 and CD44 in

Among the 627 mutually upregulated genes in the three previously mentioned groups (the MES, spliceosome-enriched, and activated NF-κB groups of TCGA GBM samples), we found several functionally defined splicing factors, including PTBP1 and SNRBP2 (Supplementary Table S2), which are reported as oncogenes in GBM.[22] We further screened 627 genes and searched for differentially expressed novel potential splicing regulators in 3 PN GBM cell lines (primary patient-derived GSC lines: NFH-GSC7, NFH-GSC8, and NFH-GSC9) and 5 MES GBM cell lines (3 primary patient-derived GSC lines: NFH-GSC1, NFH-GSC2, and NFH-GSC3; 2 established GBM cell lines: LN229 and U87MG) (Supplementary Table S3), with available transcription profiles. Representative MES and PN subtype signatures[3] are shown in the heatmap (Figure 1B, Supplementary Table S4). RSRP1 caught our attention, as its RS domain suggests that it is likely to be involved in splicing regulation; RSRP1 was significantly upregulated in MES cell lines compared with PN cell lines (3.05-fold, $P < .01$) (Figure 1B).

To further investigate whether RSRP1 contributes to the promotion of a more malignant glioma phenotype, we studied the relationship between the RSRP1 expression level and glioma grade by IHC and WB of glioma tissue samples from patients and in silico analyses of public datasets. First, IHC confirmed that RSRP1 was located in the nucleus (Figure 1C). The RSRP1 protein expression level was higher in glioma samples than in normal brain samples (grade II: 1.726-fold; grade III: 5.096-fold; Grade IV: 6.569-fold) and was positively related to glioma grade ($P < .0001$) (Figure 1D). As the RSRP1 gene is located on chromosome arm 1p, RSRP1 expression was lower in 1p/19q codeletion samples than in samples without this codeletion ($P < .0001$) (Figure 1E). In glioma tissue samples, RSRP1 expression was positively related to CD44 expression (Figure 1E), which is an MES subtype and NF-κB activation marker.[21] However, RSRP1 expression did not seem to correlate with the age, sex, or IDH status of glioma patients (Supplementary Table S5). We also assessed RSRP1 expression in 10 GBM cell lines (Supplementary Table S3) by WB. We found that RSRP1 was expressed in all of the GBM cell lines and was significantly higher in MES lines than in PN lines (Figure 1F). The stemness of 6 GSCs (NFH-GSC1, NFH-GSC2, NFH-GSC3, NFH-GSC7, NFH-GSC8, NFH-GSC9) was validated by analyzing GSC markers (SOX2, SOX9, and CD133) and pericyte/mesenchymal stem cell (MSC) markers (CD105) using IF (Supplementary Figure S1C). Moreover, intracranial tumorigenesis assays verified the tumorigenic ability of these GSCs (Figure 3B, Supplementary Figure S1C).

To further investigate the correlation between RSRP1 expression (according to IHC data) and glioma prognosis, we conducted Kaplan–Meier survival analysis with 139 glioma samples (58 GBM samples and 81 LGG samples) obtained from patients at NFH. Elevated RSRP1 expression was significantly associated with an unfavorable prognosis in glioma patients (GBM: $P < .0001$, LGG: $P = .0089$, glioma: $P < .0001$) (Figure 1G, Supplementary Figure S1A and B). Moreover, within the cohort of LGG patients with identical IDH status, high RSRP1 expression was also related to poor prognosis (IDH-WT: $P = .013$, IDH-MT: $P = .029$) (Supplementary Figure S1A). Univariate and multivariate Cox regression analyses demonstrated that RSRP1 expression was an independent risk factor in terms of glioma patient prognosis (Supplementary Table S6). We also conducted an in silico analysis of glioma samples in two public glioma datasets (GSE16011 and a TCGA dataset). Consistently, increased RSRP1 expression was also correlated with a more unfavorable prognosis in the public datasets (GSE16011: $P = .037$; TCGA: $P < .0001$) (Supplementary Figure S1B). Taken together, these results indicate that RSRP1 is a marker of an unfavorable glioma prognosis.

RSRP1 Silencing Impairs the MES Phenotype in GBM

Prompted by the above results, we studied whether RSRP1 promoted the MES phenotype in GBM. We first knocked down RSRP1 expression in 2 MES GBM cell lines (LN229 and NFH-GSC1) and 1 CL GBM cell line (T98G) with siRNAs (siRSRP1) (Figure 2A, Supplementary Figure S2A). In all cell lines, RSRP1 downregulation significantly decreased cell viability by increasing cell apoptosis, while the cell cycle was negligibly affected (Figure 2B–D, Supplementary Figure S2B). Moreover, a Transwell assay confirmed that RSRP1 knockdown impaired the invasive ability of GBM cells (Figure 2E, Supplementary Figure S2C). CD44 and p-p65 levels were also significantly decreased in RSRP1 knockdown cells, supporting that RSRP1 are involved in NF-κB activation (Figure 2A, Supplementary Figure S2A). Moreover, the observed alterations in apoptosis-related markers (cleaved PARP and cleaved caspase 3) and invasion-related markers (ZEB1, N-cadherin, E-cadherin, vimentin, and MMP-9) further supported a role for RSRP1 in maintaining the MES phenotype (Figure 2A, Supplementary Figure S2A). We also conducted rescue experiments by transfecting lentiviruses expressing shRNA-resistant mutants of RSRP1 (RSRP1-R1 or RSRP1-R2) or control vectors in RSRP1 knockdown cells (shRSRP1-1 or shRSRP1-2). RSRP1 restoration in LN229 and NFH-GSC1 cells significantly rescued the MES phenotype, as indicated by the MES marker (VIM, CD44, p-p65) expression levels (Supplementary Figure S2D).

We next explored the biological function of RSRP1 using shRSRP1 lentivirus-infected LN229 and NFH-GSC1 cells in

normal brain (NB), low-grade glioma (LGG), and GBM samples. Scale bars = 100 μm (main images) and 10 μm (insets). (D) Comparison of RSRP1 IHC staining scores among NB and different grade glioma samples. Mann–Whitney U tests were used for statistical analysis. (E) Left: Western blotting (WB) of RSRP1 and CD44 in glioma samples. Middle: Relative RSRP1 expression level in 1p/19q noncodeletion versus codeletion samples. Student's *t* test was used for statistical analysis. Right: Correlation between RSRP1 and CD44 expression based on WB results. Pearson correlation analysis was used for statistical analysis. (F) WB analysis of RSRP1 in the indicated GBM cell lines. β-Actin was used for normalization. (G) Survival curves of glioma patients stratified by RSRP1 expression. An IHC staining score of 6 was regarded as the threshold for "high expression" and "low expression" of RSRP1. Left: GBM patients; Right: LGG patients. Log-rank tests were used for survival analysis. *$P < .05$, **$P < .01$, ***$P < .001$.

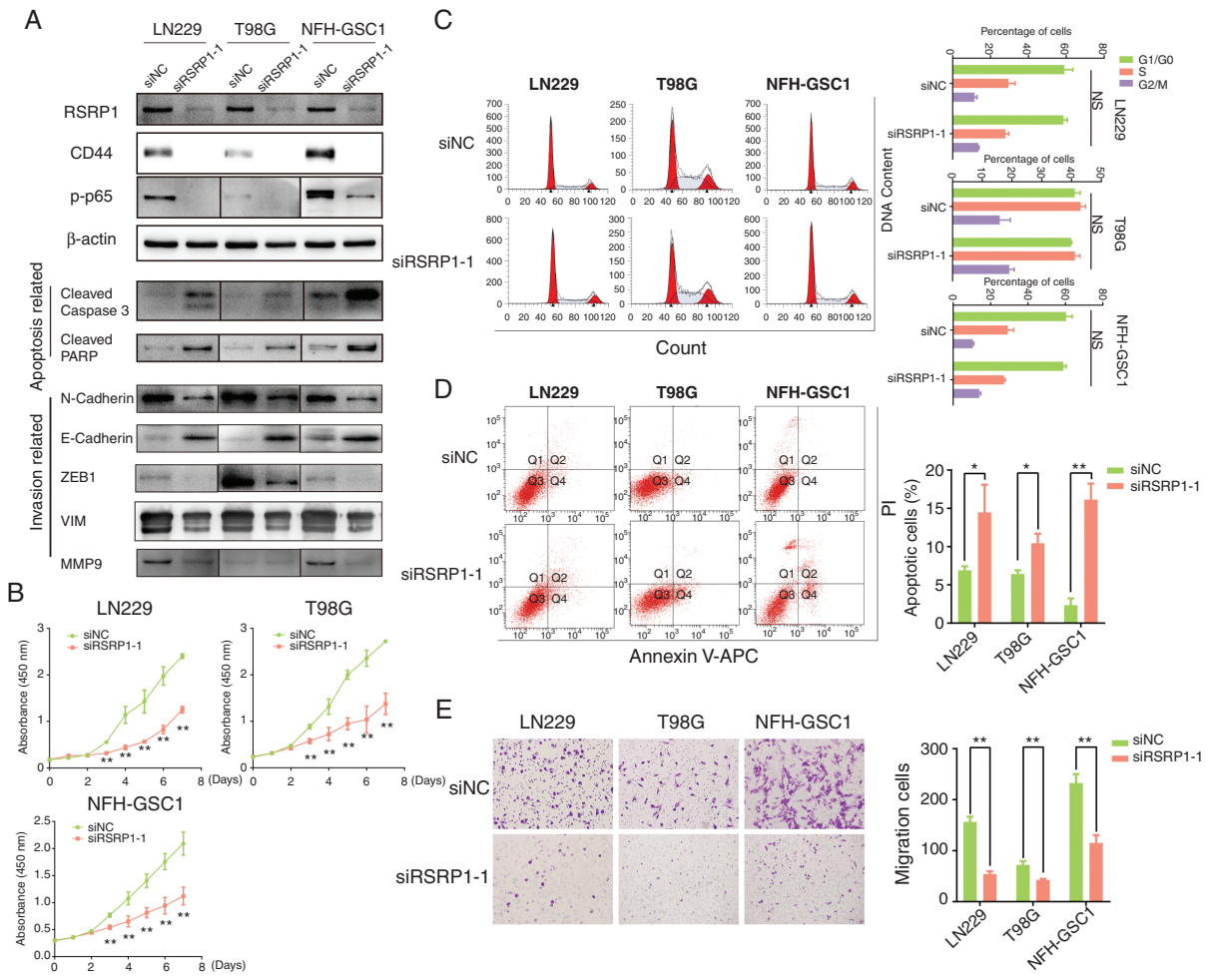

Fig. 2 In vitro assays revealed that RSRP1 is essential for GBM tumorigenesis and progression. (A) WB analysis of RSRP1, CD44, p-p65, apoptosis-related markers (cleaved caspase-3, cleaved PARP), and invasion-related markers (N-cadherin, E-cadherin, ZEB1, vimentin, and MMP-9) in the LN229, T98G, and NFH-GSC1 cell lines after transfection with the indicated siRNA. β-Actin was used for normalization. (B) Cell counts of surviving LN229, T98G, or NFH-GSC1 cells 7 days after the indicated siRNA transfection. Five technical replicates were performed for each group. Student's *t* test was used for statistical analysis. (C–D) Representative FACS plots of cell cycle analysis (C) and cell apoptosis analysis (D) in LN229, T98G, and NFH-GSC1 cell lines after the indicated siRNA transfection. Three technical replicates were performed for each group. Student's *t* test was used for statistical analysis. (E) Transwell assays of LN229, T98G, and NFH-GSC1 cell lines after transfection with the indicated siRNA. Original magnification, 400×. Five random fields of view were captured for each group. Student's *t* test was used for statistical analysis. Five technical replicates were performed for each group. One-way ANOVA was used for statistical analysis. **P* < .05. ***P* < .01. ****P* < .001. NS, not significant.

in vivo subcutaneous and intracranial tumorigenesis assays. Subcutaneous xenografts in nude mice derived from GBM cells transfected with shRSRP1-1 had significantly lower mean weights than those derived from control cells (Figure 3A). Furthermore, MRI and hematoxylin and eosin (HE) staining of intracranial tumor-bearing mice at 3 weeks after implantation suggested that compared with the control conditions, RSRP1 knockdown impaired tumor growth (Figure 3B, Supplementary Figure S2E). Importantly, RSRP1 knockdown reduced the progression of xenograft tumor growth and prolonged overall survival in nude mice bearing intracranial tumors (*P* < .001) (Figure 3D). A reduction in the MES signature genes (vimentin, p-p65) and an increase in TUNEL staining positivity were observed in tumors with downregulated RSRP1 (Figure 3C). However, the expression of a proliferation marker (Ki67) did not differ between the control and RSRP1 knockdown groups (Figure 3C), suggesting that the suppression of tumor growth after RSRP1 silencing resulted from increased apoptosis and decreased invasion. Collectively, these in vivo and in vitro experiments revealed that RSRP1 is essential for maintaining the MES phenotype in GBM.

RSRP1 is Associated with Spliceosome Factors via Serine Phosphorylation

To determine how RSRP1 exerts its intriguing function of regulating the MES phenotype, we further explored the molecular function of RSRP1. Given that RSRP1 is enriched with arginine (R) and serine (S), it is probable that it regulates splicing by mediating interactions among splicing factors.[23] To confirm the biological function of RSRP1 as an SR-related protein, we first performed proteomic assays to identify RSRP1-interacting proteins. We transfected an RSRP1-wild-type (WT)-FLAG-EGFP lentivirus vector into LN229 GBM cells and subsequently performed Co-IP followed by mass spectrometry (Co-IP-MS).

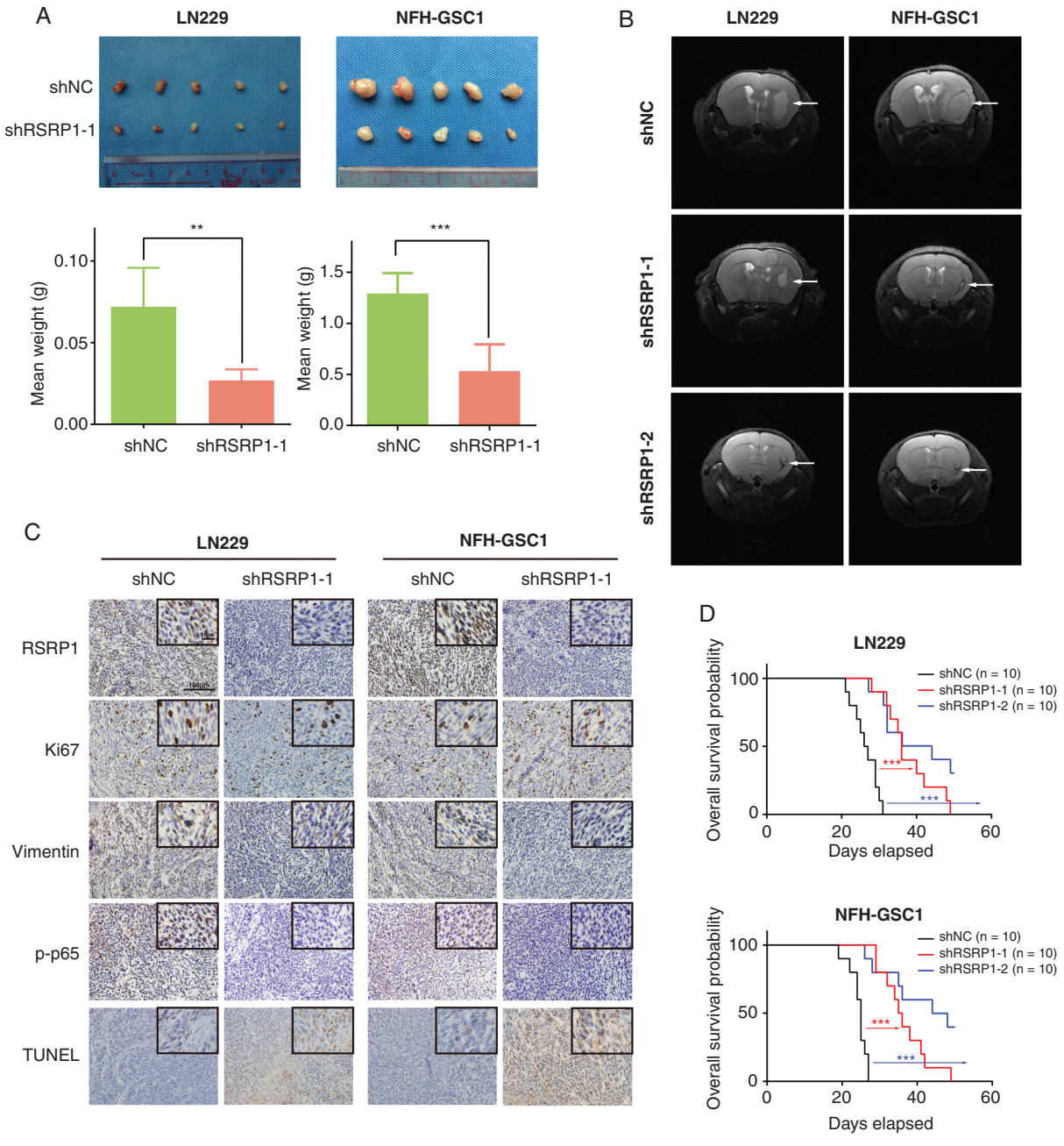

Fig. 3 In vivo assays reveal that RSRP1 is essential for glioblastoma tumorigenesis and progression. (A) Top: Images of subcutaneous xenograft tumors of stable shRNA-transfected LN229 or NFH-GSC1 cells collected from nude mice. Bottom: The mean weights of xenograft tumors in the shRNA groups. Five technical replicates were performed for each group. Student's *t* test was used for statistical analysis. (B) Representative cranial MRI T2 sequence images of intracranial tumor-bearing mice 3 weeks after transplantation for each shRNA group. (C) HE staining and IHC staining of xenograft tumors in different shRNA groups. Scale bars = 100 μm and 10 μm. (D) Survival curves of intracranial tumor-bearing mice in each shRNA group. Ten technical replicates were performed for each group. $^{**}P < .01$. $^{***}P < .001$.

Most of the RSRP1-related proteins in the RSRP1-WT-transfected group were spliceosomal proteins, while this pattern was not observed for the control group (Figure 4A, Supplementary Table S7). Specifically, the identified RSRP1-related proteins were primarily enriched for the "RNA splicing," "RNA binding" and "spliceosomal snRNP complex" terms based on gene ontology (GO) analysis (Supplementary Figure S3A) and were enriched for the "spliceosome" term according to Kyoto Encyclopedia of Genes and Genomes (KEGG) pathway analysis (Supplementary Figure S3B). We verified several RSRP1-related proteins, including those in the core spliceosomal subcomplex at different stages of the splicing cycle (U1 snRNP: SNRPA; U2 snRNP: SF3B1; tri-snRNP: SART1; Sm proteins: SNRPF; NTC: PRPF19; hnRNPs: HNRNPC; BCLAF1; and splicing kinase: CLK2), by WB, IF and bimolecular fluorescence complementation (BiFC) (Figure 4B and C, Supplementary Figure S3C). We found that RSRP1 interacted with many core spliceosomal proteins, indicating that RSRP1 is present during several stages of spliceosome assembly in GBM cells.

To identify the key RSRP1 domain that contributes to the interactions with spliceosomal proteins, we constructed four RSRP1 mutants (RSRP1-Δ1-60aa, RSRP1-Δ60-160aa, RSRP1-Δ160-240aa, and RSRP1-Δ240-290aa) and then evaluated their ability to bind spliceosomal proteins through Co-IP (Figure 4D and E). We found that RSRP1-Δ1-60aa, RSRP1-Δ160-240aa, and RSRP1-Δ240-290aa could all bind the spliceosomal proteins in a similar manner to RSRP1-WT, but RSRP1-Δ60-160aa could not (Figure 4F). This finding indicates that the key RSRP1 domain involved in the interaction with the spliceosome lies within aa 60-160.

Generally, splicing factor interactions depend on the phosphorylation of serine residues in the RS domain.[24] Thus, we used PhosphoSitePlus (https://www.phosphosite.org/homeAction.action) to predict the phosphorylation site that contributes to protein binding. Within RSRP1 60-160aa, S107, and S109 were the most likely phosphorylation sites. We constructed three additional RSRP1 mutants, RSRP1-S107A, RSRP1-S109A, and RSRP1-S107A/S109A, to prevent phosphorylation at these sites. The ability of RSRP1-S107A and RSRP1-S109A to bind spliceosome proteins was similar to that of RSRP1-WT; however, combined mutation of both S107 and S109 dramatically weakened the interactions between RSRP1 and spliceosome proteins (Supplementary Figure S3D). Collectively, our data indicate that RSRP1 is a novel SR-related protein that interacts with various spliceosome proteins via phosphorylated S107 and S109 sites.

RSRP1 Promotes NF-κB Activation by Regulating Splicing in MES GBM

To gain insight into the mechanism by which RSRP1 regulates splicing, we attempted to analyze RNA-seq results for RSRP1-regulated AS in MES GBM cells. We transfected RSRP1-WT or control lentiviruses into LN229 and NFH-GSC1 cell lines and verified the level of overexpression by WB. RNA-seq analyses were then conducted for RSRP1-overexpressing/control LN229/NFH-GSC1 cell lines. By AS analysis, we identified a substantial alteration in splicing events after RSRP1 overexpression. Specifically, we observed 4,091 events in LN229 cells and 4,270 events in NFH-GSC1 cells ($n = 3$, $\Delta PSI > 0.15$, FDR < 0.05) (Figure 5A). Most of the RSRP1-regulated AS events were exon-skipping (SE) events (67% in LN229 cells, 67% in NFH-GSC1 cells) (Figure 5A), and a decreased percent spliced-in index (PSI) for RSRP1-regulated AS was observed in SE events (59% in LN229 cells, 63% in NFH-GSC1 cells) (Figure 5B). We found 210 decreased PSIs and 102 increased PSIs of SE events in the LN229 and NFH-GSC1 cell lines, respectively (Figure 5C, Supplementary Tables S8–S9).

We next verified the top 40 RSRP1-regulated decreased PSIs of SE events by RT-PCR (Supplementary Table S8). Representative results of 5 validated AS events were shown, including a reported protumorigenic AS event: exon 7 skipping in EXOC7[25] (Figure 5D). Moreover, we also identified the isoform switch of PARP6, a reported tumor suppressor in colorectal cancer[26,27] that thus far has not been studied in the context of glioma. RSRP1 overexpression in glioma cells caused exon 18 skipping in PARP6 (Figure 5D, Supplementary Figure S4A). Compared to the full-length isoform (PARP6-fl), the truncated isoform (PARP6-s) lacked a 113-bp region in exon 18, causing a frameshift mutation and PARP catalytic triad (histidine-tyrosine-isoleucine, HYI) deficiency (Figure 5E). Based on in silico analyses and the validation of tissue samples through RT-PCR, we found the following results: (1) the predominant PARP6 isoform in brain and glioma tissues was PARP6-fl (Figure 5F and G); (2) there was a higher proportion of PARP6-s in glioma samples than in normal brain samples (Figure 5F and G); (3) the level of PARP6-s was associated with the tumor grade (Figure 5F and G); (4) a high level of PARP6-s in glioma indicated a poor prognosis (Figure 5H); and (5) the PSI values of PARP6 exon 18 were negatively related to the RSRP1 levels in TCGA glioma samples ($P < .001$) (Supplementary Figure S4B). Collectively, these data indicate that PARP6-s might play a role in determining the malignant phenotype of glioma.

The RSRP1-Regulated PARP6 Isoform Switch Activates NF-κB by Promoting NEMO Ubiquitylation

Prompted by the above findings, we further explored how the RSRP1-regulated PARP6 isoform switch contributed to NF-κB activation. Interactome analysis (https://thebiogrid.org/) has shown that potential PARP6 interactors are involved in the NF-κB pathway,[28,29] including p47 (also known as NSFL1C), which interacts with the essential NF-κB regulator IκKγ (NEMO).[29] Previous studies revealed that ADP-ribose polymerases (PARP9, PARP10) precluded ubiquitylation through ADP-ribosylation[30,31]; in particular, PARP10 inhibited NF-κB activation by interfering with the polyubiquitination of NEMO, which was dependent on catalytic activity.[31] This evidence guided us to hypothesize that PARP6 regulates NF-κB activation by interacting with p47 and participating in NEMO ubiquitination in a manner dependent on the catalytic triad.

Consistent with our previous data, WB data indicated that RSRP1 induced NF-κB activation through the canonical

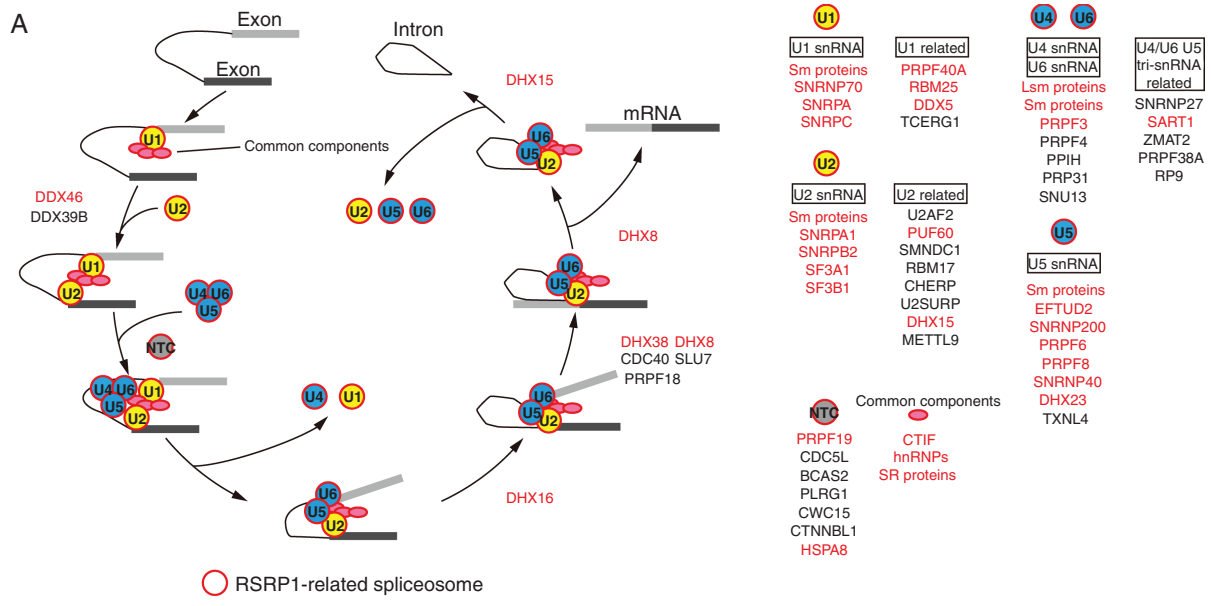

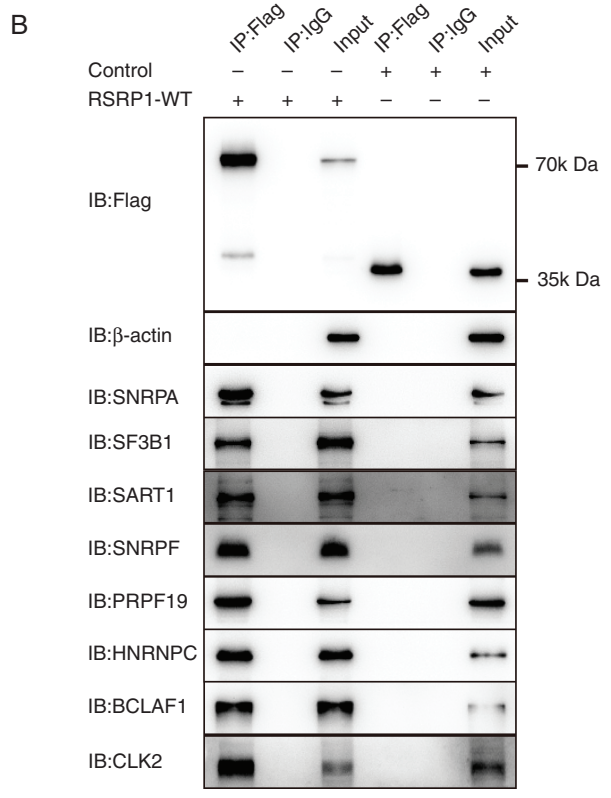

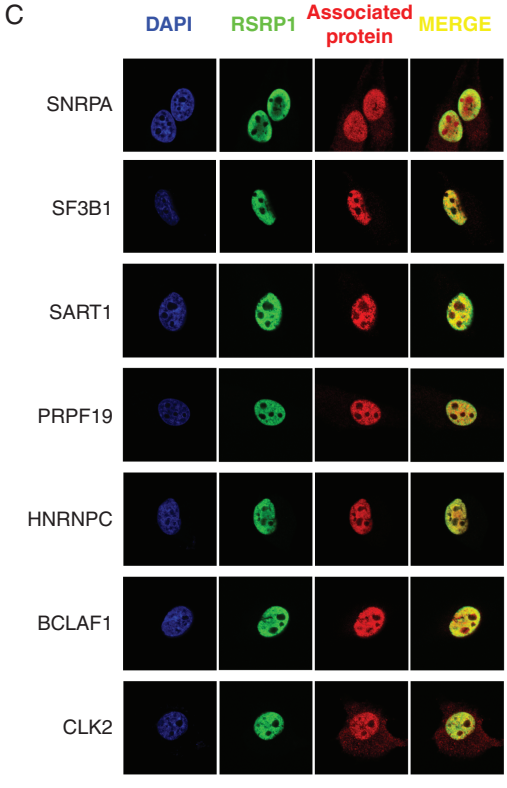

Fig. 4 RSRP1 is associated with various spliceosome-related factors. (A) Schematic diagram of RSRP1-associated spliceosome factors in the splicing cycle based on mass spectrometry assays. Spliceosomal snRNPs (red circle) and proteins (red) interacting with RSRP1 are marked. (B) RSRP1-Flag Co-IP of core spliceosomal factors. (C) Representative immunofluorescence (IF) staining showing the colocalization of RSRP1 and core spliceosomal factors in LN229 cells. (D) Left: Schematic of the wild-type RSRP1 (RSRP1-WT) amino acid sequence. Right: Schematics of truncated RSRP1 mutants (RSRP1-Δ1-60aa, RSRP1-Δ60-160aa, RSRP1-Δ160-240aa, and RSRP1-Δ240-290aa). (E) Left: WB analysis of exogenous RSRP1-WT and RSRP1 mutant expression. Right: RSRP1 mutant coimmunoprecipitation (Co-IP) with core spliceosomal factors.

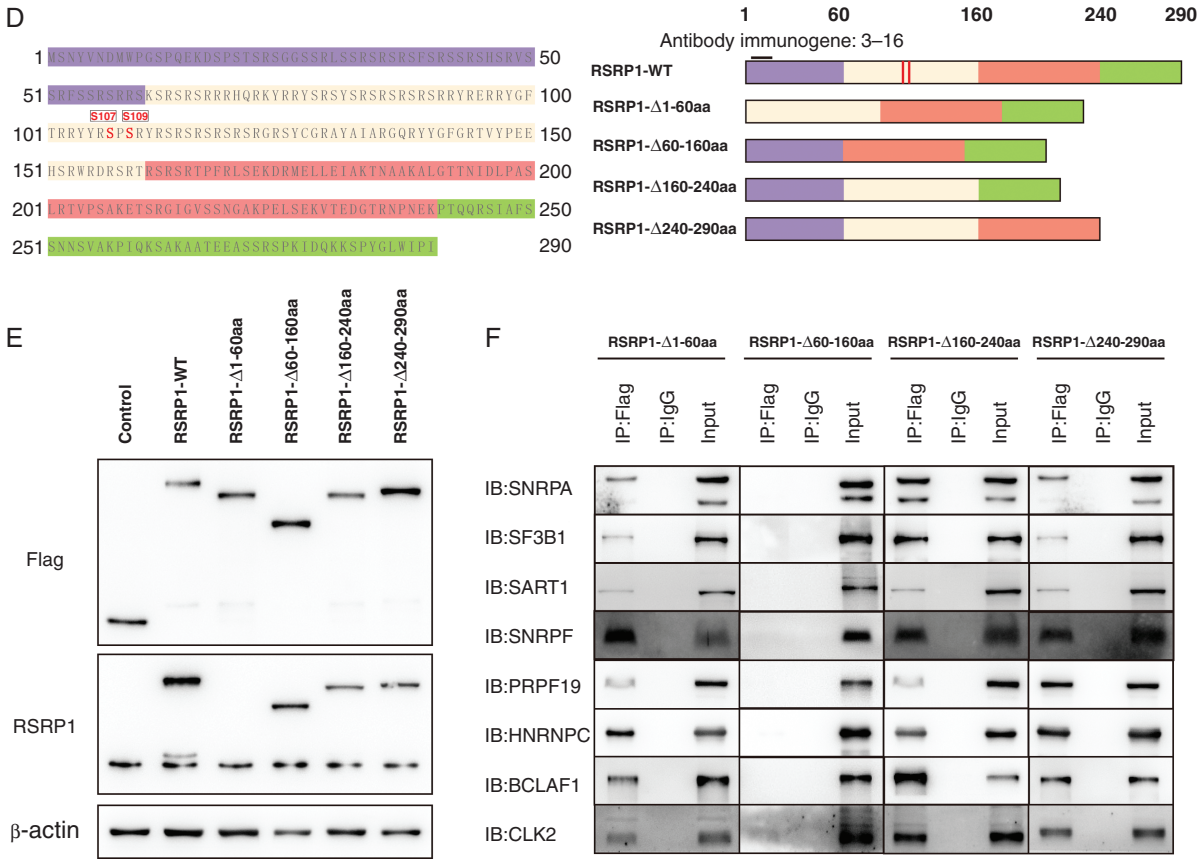

Fig. 4 (Continued)

NF-κB pathway by upregulating p-IκBα expression (Figure 5I). To confirm that PARP6 isoform switch-mediated NF-κB activation depends on the p47 interaction, we constructed PARP6-fl- and PARP6-s-infected LN229 cells and conducted an IP assay. IP analysis showed that PARP6-fl bound to p47 and NEMO, while PARP6-s lacked this ability (Figure 5J), which suggested that PARP6 interacts with p47 and inhibits the ubiquitination of NEMO and that these actions are dependent on the catalytic triad; thus, the RSRP1-regulated PARP6 isoform switch promotes the ubiquitination of NEMO.

Another core spliceosomal factor related to the U2 snRNP, SF3B1, is one of the best known spliceosome targets[32]; SF3B1 was also verified to be associated with RSRP1 through IP analysis, IF analysis, and BiFC assay (Figure 4B). Our bioinformatic analysis of POSTAR2 (http://lulab.life.tsinghua.edu.cn/postar/rbp2.php) based on cross-linking immunoprecipitation (CLIP) assays showed that SF3B1 could bind PARP6 (Supplementary Table S10). Thus, we next conducted RT-PCR to examine whether SF3B1 contributes to the PARP6 isoform switch. Our data showed that interference with SF3B1 in LN229 and NFH-GSC1 cells resulted in a reduction in the level of PARP6-s (Figure 5K). This finding is consistent with the hypothesis that RSRP1 regulates the AS of PARP6 by interacting with spliceosome factors. Taken together, our data show that the PARP6-fl and p47 complex interacts with NEMO and inhibits NEMO ubiquitination, suppressing the NF-κB pathway. Without the catalytic triad, PARP6-s loses the ability to regulate NEMO ADP-ribosylation, causing NEMO ubiquitination and further NF-κB activation.

RSRP1 Promotes the GBM MES Phenotype by Regulating PARP6 Splicing and NF-κB Activation

We next conducted recovery experiments to further validate the above results. We used the CRISPR/Cas9 genome editing system to construct RSRP1-KO MES GBM cell lines (LN229 and NFH-GSC1) (Supplementary Figure S6A). Then, to confirm the mechanism through which RSRP1 promotes the GBM MES phenotype, we performed recovery experiments by stably transfecting various lentiviruses (including a control vector, RSRP1-WT, RSRP1-S107A/S109A, PARP6-s, and PARP6-fl) into these KO cells and analyzing MES phenotype-related signatures and biological functions. First, WB showed that the levels of NF-κB activation markers (p-IκBα and p-p65)

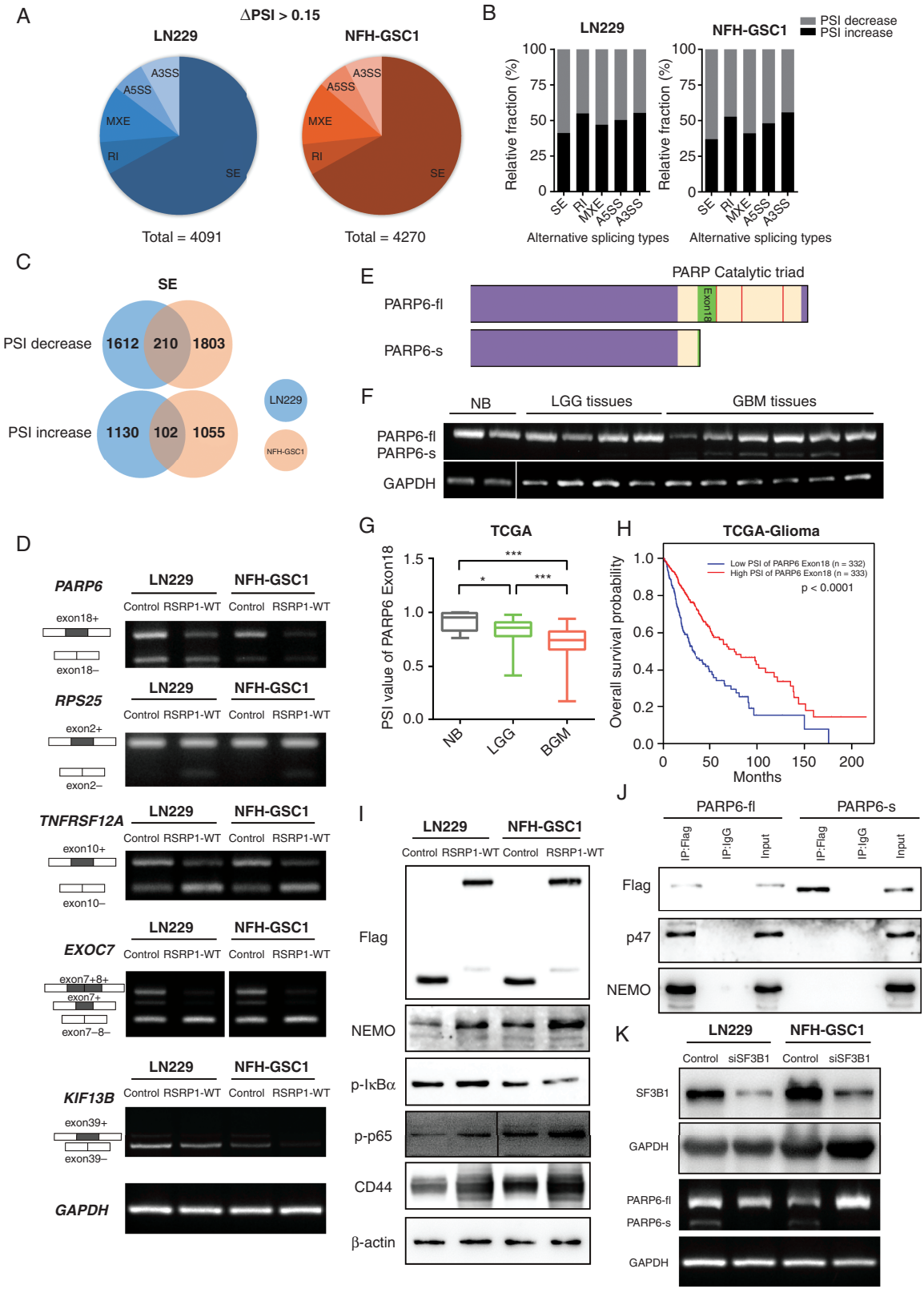

Fig. 5 RSRP1 participates in NF-κB activation through splicing regulation. (A) RSRP1-regulated AS in LN229 and NFH-GSC1 cells. SE: skipped exon, RI: retained intron, A5SS: alternative 5′ splice site, A3SS: alternative 3′ splice site, MXE: mutually exclusive exon. (B) Alterations in percent spliced-in index (PSI) values in different splicing categories after RSRP1 overexpression in LN229 or NFH-GSC1 cells. (C) Venn diagrams showing

and CD44 were significantly decreased after RSRP1 KO in LN229 and NFH-GSC1 cells (Supplementary Figure S6A). Exogenous expression of RSRP1-WT or PARP6-s but not RSRP1-S107A/S109A or PARP6-fl restored the downregulation of the expression of these MES markers (Supplementary Figure S6A). Transwell assays and flow cytometry showed that exogenous expression of RSRP1-WT or PARP6-s but not RSRP1-S107A/S109A or PARP6-fl also attenuated the suppression of migration and apoptosis resistance caused by RSRP1 KO (Supplementary Figure S6B and C). These data further suggest that RSRP1 activates the NF-κB pathway by regulating PARP6 splicing.

Coincidentally, intracranial xenograft assays showed that RSRP1-KO GBM cells showed marginal tumorigenesis, while RSRP1-WT or PARP6-s, but not RSRP1-S107A/S109A or PARP6-fl, transfection restored xenograft growth (Figure S5, Supplementary Figure S6D and E). These findings support that RSRP1 promotes the GBM MES phenotype by regulating PARP6 splicing and NF-κB activation.

Targeting Spliceosomes and the NF-κB Pathway Is a Feasible Treatment for MES GBM

Our experimental data suggest that RSRP1 contributes to GBM malignancy through its roles in spliceosome assembly and the NF-κB pathway. We further performed survival analysis on the Chinese Glioma Genome Atlas (CGGA) dataset stratified by the expression level of RSRP1-associated spliceosomes, including SF3B1 and CLK2. SF3B1 and CLK2 expression was observed to be related to poor clinical outcomes (SF3B1: $P = .0037$; CLK2: $P = .0038$) (Figure 6A). This finding provided a basis for exploring the efficacy of a treatment for GBM that simultaneously targets spliceosomes and the NF-κB pathway due to the crucial roles of both processes in MES GBM. We chose two spliceosome inhibitors [one targeting SF3B1 (pladienolide B) and one targeting CLK2 (TG003)] and two NF-κB inhibitors (BAY11-7082 and DHMEQ) for our pharmacological analyses. Pladienolide B is an effective spliceosome inhibitor that impairs the U2 snRNP interaction with pre-mRNA.[33] TG003 regulates AS by inhibiting SR protein phosphorylation.[34] BAY11-7082 and DHMEQ are specific NF-κB inhibitors that target IκK and p65, respectively, and have already been reported to be effective drugs for GBM.[35] We used LN229, NFH-GSC1, and the corresponding RSRP1-KO cell lines (LN229-KO and NFH-GSC1-KO) as models in these pharmacology experiments. All cell lines responded to each drug individually (Figure 6B, Supplementary Figure S7A). Interestingly, the RSRP1-KO cell lines were more sensitive to all four inhibitors than were their parental cell lines (Figure 6B, Supplementary Figure S7A), further demonstrating the role of RSRP1 in spliceosomes and the NF-κB pathway. Moreover, the 4 drugs decreased the expression levels of MES markers (VIM, CD44, p-p65) in LN229 and NFH-GSC1 cells, indicating the inhibitory effects of spliceosome inhibitors and NF-κB inhibitors on MES GBM (Figure 6D, Supplementary Figure S7B).

Next, we evaluated the effect of combinatorial treatments on GBM cell lines by pairing one spliceosome inhibitor with one NF-κB inhibitor. A synergistic effect was observed in both the LN229 cell line and the NFH-GSC1 cell line in each combination treatment group, with ZIP synergy scores >1 (LN229: 2.414-6.685; NFH-GSC1: 3.13-7.55) (Figure 6C, Supplementary Figure S7C). In vitro assays revealed that the combination of pladienolide B (1 nM) and BAY11-7082 (20 μM) suppressed NF-κB activation and decreased the viability of MES GBM cells (LN229 and NFH-GSC1) more dramatically than either drug alone ($P < .001$) (Figure 6D and E).

Finally, we conducted in vivo assays to evaluate the efficacy of combined spliceosome and NF-κB inhibitor treatment against MES GBM. We implanted NFH-GSC1 cells into the right cerebral cortex of nude mice, and 10 days after implantation, we intraperitoneally injected the tumor-bearing mice with the vehicle, 10 mg/kg pladienolide B, 2.5 mg/kg BAY11-7082 or a premixed combination of 10 mg/kg pladienolide B and 2.5 mg/kg BAY11-7082 twice weekly for 3 weeks. Inhibition of tumor growth, angiogenesis, and MES signatures (vimentin, CD44, p-p65) was observed in tumors treated with pladienolide B or BAY11-7082 based on the HE staining and IHC results (Figure 6F and G, Supplementary Figure S8). Treatment with a combination of two drugs inhibited tumor growth to a greater extent than either agent alone (Figure 6F and G, Supplementary Figure S8). The tumor-bearing mice ($n = 5$ per group) administered a single drug had significantly longer survival than the mice administered the vehicle control ($P < .05$), while those administered the combination treatment showed the best outcome ($P < .01$) (Figure 6H). In conclusion, in vitro, and in vivo assays revealed that combined spliceosome and NF-κB inhibition synergistically reduced GBM growth. Taken together, these results suggest that targeting spliceosomes and the NF-κB pathway is a feasible combinatory treatment for MES GBM.

AS events with increased PSI and decreased PSI values after RSRP1 overexpression in LN229 or NFH-GSC1 cells. (D) Representative validation of RSRP1-regulated AS. (E) Schematic of the PARP-fl and PARP-s isoforms. Red lines represent the "HYI" triad. (F) RT-PCR analysis of the PARP-fl and PARP-s isoform levels in NB, LGG, and GBM tissues. (G) PSI values of PARP6 exon 18 in NB, LGG, and GBM tissues. (H) Survival curves of glioma patients in TCGA datasets. The median PSI value was regarded as the cutoff between high and low levels of PARP6 exon 18. The log-rank test was used to calculate the *P*-value. (I) WB analysis of downstream NF-κB pathway components after RSRP1 overexpression in LN229 or NFH-GSC1 cells. (J) PARP6-fl and PARP6-s Co-IP with p47 and NEMO. (K) WB analysis of SF3B1 and PARP6 isoform expression levels after SF3B1 knockdown. GAPDH was used for normalization. $^{*}P < .05$. $^{***}P < .001$.

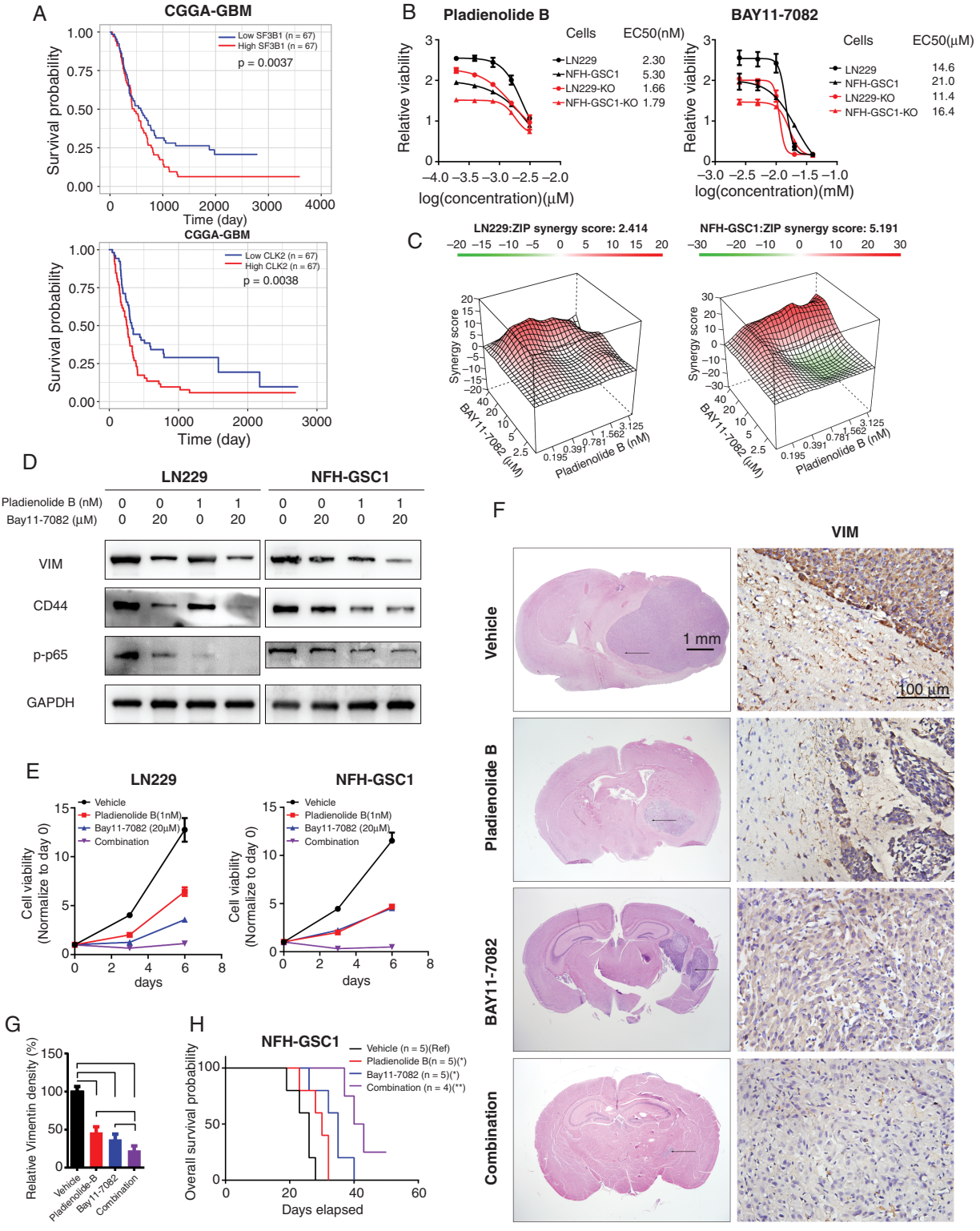

Fig. 6 Targeting spliceosomes and the NF-κB pathway is a feasible treatment for MES GBM. (A) Survival curve analysis of GBM patients in the CGGA database stratified by the expression of SF3B1 and CLK2. Log-rank tests were used for survival analysis. (B) The concentration-response curves and half-maximal effective concentration (EC50) values of pladienolide B or BAY11-7082 in the LN229, NFH-GSC1, and corresponding RSRP1-KO cell lines (LN229-KO and NFH-GSC1-KO). Three technical replicates were performed for each group. (C) The synergy scores for the pladienolide B and BAY11-7082 combinations in LN229 (left) and NFH-GSC1 (right) cell lines were calculated by using the SynergyFinder platform (https://synergyfinder.fimm.fi/). (D) WB analysis of vimentin, CD44, and p-p65 in LN229 and NFH-GSC1 cell lines after treatment with pladienolide B

Discussion

To determine how spliceosome factors regulate the GBM MES phenotype, we first conducted a bioinformatic analysis to screen for essential factors and ultimately focused on RSRP1. Interestingly, our bioinformatic analysis indicated that the spliceosome might promote the MES phenotype of GBM almost exclusively via the NF-κB pathway; this finding was based on the detection of the mutually upregulated spliceosome and NF-κB markers in the TCGA GBM dataset and was also one of the theoretical bases of the underlying synergistic effect achieved by targeting the spliceosome and NF-κB pathway.

RSRP1 is a novel SR-related protein belonging to a superfamily of proteins composing the spliceosome complex. Previous studies have suggested that SR-related proteins have essential roles in the central nervous system (CNS).[36] However, despite increasing evidence that splicing factors participate in tumorigenesis and GBM progression, the roles of SR-related proteins without an RNA recognition motif (RRM) are unclear. Based on our in vitro and in vivo analyses, we propose that RSRP1 regulates GBM malignancy through the phosphorylation of its RS domain, which allows it to interact with splicing factors; it also contributes to spliceosome assembly and ultimately regulates splicing progression.

A recent study found that in breast cancer, one SR protein, BUD31, functions by assembling multiple spliceosomes, which is similar to the function of RSRP1,[16] indicating the importance of this mechanism in cancer. Targeting this kind of assembly protein might, therefore, be an effective method for generally targeting spliceosome factors in cancer.

RNA-seq analysis showed that AS was markedly affected by RSRP1. We studied the AS of PARP6 in detail, as PARP6 is one of the functional executors in RSRP1-guided MES phenotype promotion. The PARP protein family functions through a catalytic triad, although the precise nature of the catalytic triad differs among different PARPs.[37] Although there is evidence suggesting that PARP6 is a tumor suppressor and that a PARP6 isoform that lacks the catalytic triad promotes cancer progression,[27] the upstream and downstream molecular mechanisms of PARP6 isoform formation remain unknown. Here, we identified the splicing regulatory mechanism underlying this PARP6 isoform switch: RSRP1-regulated exon 18 skipping results in PARP6 catalytic triad deletion in GBM. This pathogenic isoform enhances NF-κB activation and promotes the MES GBM phenotype. We also observed RSRP1-regulated AS causes exon 7 skipping in EXOC7, which is a known oncogenic AS event causing the senescence-associated secretory phenotype (SASP).[25] Whether EXOC7 exon 7 skipping and the SASP contribute to the MES phenotype requires further research.

Given that we showed that spliceosomes promote the MES phenotype through NF-κB activation, we conducted therapeutic experiments with drugs targeting spliceosome factors and the NF-κB pathway. Although NF-κB-targeting drugs have been well studied in GBM and other cancers,[32] intensive research on pharmacological treatments targeting the spliceosome in GBM has not been performed. In this study, we used pladienolide B (targeting SF3B1)[32] and TG003 (targeting CLKs),[34] two well-studied spliceosome inhibitors, as treatments for MES GBM and found a synergistic effect when spliceosome- and NF-κB-targeting drugs were combined. Furthermore, we found that RSRP1-KO GBM cells were more sensitive to spliceosome- and NF-κB-targeting drugs than WT GBM cells, indicating the role of RSRP1 in spliceosome-regulated NF-κB activation. Pladienolide B and BAY11-7082 were applied as spliceosome- and NF-κB-targeting drugs, respectively, in this study and showed treatment effects for MES GBM based on in vivo and in vitro assays and exhibited safety in previous preclinical studies.[6,38] Since MES transition occurs in treatment-resistant GBM cases,[7] this spliceosome- and NF-κB-targeting combinatory strategy might be promising for patients with recurrent disease. Moreover, according to our data, patients with spliceosome-enriched or RSRP1-overexpressing GBM might be suited for such modalities.

This study might also provide a new perspective for diseases other than GBM. NF-κB activation has been recognized as a molecular hallmark related to chronic inflammation,[39] and the anti-inflammatory effects of spliceosome-targeting treatment are worth exploring. The MES transition is associated with the progression of multiple malignancies.[39] Future studies will define the splicing-regulated MES transition of other tumors and the potential utility of the combination strategies targeting spliceosomes and NF-κB in these cancers.

In conclusion, we have identified a novel mechanism through which spliceosomes promote the GBM MES phenotype. Our mechanistic axis centers on NF-κB pathway activation via a novel spliceosomal factor, RSRP1 (Supplementary Figure S9). We show that the skipping of exon 18 in PARP6, one RSRP1-regulated AS event, serves as a prognostic marker in GBM and is associated with MES GBM properties, as PARP6-s promotes NF-κB activation. We also found a synergistic antitumor effect on GBM for spliceosome- and NF-κB-targeting drugs, suggesting that targeting RSRP1 function might be a promising treatment for MES GBM.

(1 nM), BAY11-7082 (20 μM), or both. GAPDH was used for normalization. (E) Relative survival of LN229 and NFH-GSC1 cells after treatment with the indicated concentrations of pladienolide B (3 nM), BAY11-7082 (20 μM), or both. (F) HE staining and IHC staining of xenograft tumors treated with vehicle, 10 mg/kg pladienolide B, 2.5 mg/kg BAY11-7082, or both. Scale bar = 1 mm and 100 μm. (G) Graphic analysis of (F) shows the relative vimentin density in different cells as indicated. (H) Survival curves of intracranial tumor-bearing mice treated with vehicle, 10 mg/kg pladienolide B, 2.5 mg/kg BAY11-7082, or both. Technical replicates were performed for each group as indicated. The log-rank test was used for statistical analysis. *$P < .05$; **$P < .01$; ***$P < .001$.

Supplementary Material

Supplementary data are available at *Neuro-Oncology* online.

Keywords

glioblastoma | mesenchymal phenotype | NF-κB | RSRP1 | spliceosome

Funding

This study was supported by the National Natural Science Foundation of China (grant nos. 81773290, 81872442, and 81803100), PLA Logistics Research Project of China (CWH17L020, 18CXZ030), Outstanding Youth Development Scheme of Nanfang Hospital, Southern Medical University (2019J002).

Acknowledgments

Not applicable.

Authorship statement. Y.L.1 was the major contributor in experiments performing and manuscript writing. X.W. was the major contributor in experiments performing. Y.L.2, X.Z., and S.Q. were the contributors of the design of the study. L.G. and G.H. were the major contributors in data acquisition and specimen collection. Z.R., K.L., Y.P., G.Y., J.G., R.Y., and H.W. were contributors in experiments performing and analysis presentation.

Conflicts of interest statement. The authors declared no conflicts of interest.

References

1. Lapointe S, Perry A, Butowski NA. Primary brain tumours in adults. *Lancet.* 2018;392(10145):432–446.
2. Patel AP, Tirosh I, Trombetta JJ, et al. Single-cell RNA-seq highlights intratumoral heterogeneity in primary glioblastoma. *Science.* 2014;344(6190):1396–1401.
3. Wang Q, Hu B, Hu X, et al. Tumor evolution of glioma-intrinsic gene expression subtypes associates with immunological changes in the microenvironment. *Cancer Cell.* 2017;32(1):42–56.e6.
4. Yuan J, Levitin HM, Frattini V, et al. Single-cell transcriptome analysis of lineage diversity in high-grade glioma. *Genome Med.* 2018;10(1):57.
5. Verhaak RG, Hoadley KA, Purdom E, et al.; Cancer Genome Atlas Research Network. Integrated genomic analysis identifies clinically relevant subtypes of glioblastoma characterized by abnormalities in PDGFRA, IDH1, EGFR, and NF1. *Cancer Cell.* 2010;17(1):98–110.
6. Cahill KE, Morshed RA, Yamini B. Nuclear factor-κB in glioblastoma: insights into regulators and targeted therapy. *Neuro Oncol.* 2016;18(3):329–339.
7. Kim SH, Ezhilarasan R, Phillips E, et al. Serine/Threonine Kinase MLK4 determines mesenchymal identity in glioma stem cells in an NF-κB-dependent Manner. *Cancer Cell.* 2016;29(2):201–213.
8. Friedmann-Morvinski D, Narasimamurthy R, Xia Y, Myskiw C, Soda Y, Verma IM. Targeting NF-κB in glioblastoma: a therapeutic approach. *Sci Adv.* 2016;2(1):e1501292.
9. Cameron AR, Morrison VL, Levin D, et al. Anti-inflammatory effects of metformin irrespective of diabetes status. *Circ Res.* 2016;119(5):652–665.
10. Barbie TU, Alexe G, Aref AR, et al. Targeting an IKBKE cytokine network impairs triple-negative breast cancer growth. *J Clin Invest.* 2014;124(12):5411–5423.
11. Saba NS, Liu D, Herman SE, et al. Pathogenic role of B-cell receptor signaling and canonical NF-κB activation in mantle cell lymphoma. *Blood.* 2016;128(1):82–92.
12. Robe PA, Martin DH, Nguyen-Khac MT, et al. Early termination of ISRCTN45828668, a phase ½ prospective, randomized study of sulfasalazine for the treatment of progressing malignant gliomas in adults. *BMC Cancer.* 2009;9:372.
13. Gimple RC, Kidwell RL, Kim LJY, et al. Glioma stem cell-specific superenhancer promotes polyunsaturated fatty-acid synthesis to support EGFR signaling. *Cancer Discov.* 2019;9(9):1248–1267.
14. Dong Z, Zhang G, Qu M, et al. Targeting glioblastoma stem cells through disruption of the circadian clock. *Cancer Discov.* 2019;9(11):1556–1573.
15. Li Y, Ren Z, Peng Y, et al. Classification of glioma based on prognostic alternative splicing. *BMC Med Genomics.* 2019;12(1):165.
16. Hsu TY, Simon LM, Neill NJ, et al. The spliceosome is a therapeutic vulnerability in MYC-driven cancer. *Nature.* 2015;525(7569):384–388.
17. Lin S, Fu XD. SR proteins and related factors in alternative splicing. *Adv Exp Med Biol.* 2007;623:107–122.
18. Yi GZ, Huang G, Guo M, et al. Acquired temozolomide resistance in MGMT-deficient glioblastoma cells is associated with regulation of DNA repair by DHC2. *Brain.* 2019;142(8):2352–2366.
19. Li Y, Liu Y, Ren J, et al. miR-1268a regulates ABCC1 expression to mediate temozolomide resistance in glioblastoma. *J Neurooncol.* 2018;138(3):499–508.
20. Ceccarelli M, Barthel FP, Malta TM, et al.; TCGA Research Network. Molecular profiling reveals biologically discrete subsets and pathways of progression in diffuse glioma. *Cell.* 2016;164(3):550–563.
21. Bhat KPL, Balasubramaniyan V, Vaillant B, et al. Mesenchymal differentiation mediated by NF-κB promotes radiation resistance in glioblastoma. *Cancer Cell.* 2013;24(3):331–346.
22. Correa BR, de Araujo PR, Qiao M, et al. Functional genomics analyses of RNA-binding proteins reveal the splicing regulator SNRPB as an oncogenic candidate in glioblastoma. *Genome Biol.* 2016;17(1):125.
23. Blencowe BJ, Issner R, Nickerson JA, Sharp PA. A coactivator of pre-mRNA splicing. *Genes Dev.* 1998;12(7):996–1009.
24. Shepard PJ, Hertel KJ. The SR protein family. *Genome Biol.* 2009;10(10):242.
25. Georgilis A, Klotz S, Hanley CJ, et al. PTBP1-Mediated Alternative Splicing Regulates the Inflammatory Secretome and the Pro-tumorigenic Effects of Senescent Cells. *Cancer Cell.* 2018;34(1):85–102.e9.
26. Qi G, Kudo Y, Tang B, et al. PARP6 acts as a tumor suppressor via downregulating Survivin expression in colorectal cancer. *Oncotarget.* 2016;7(14):18812–18824.

27. Tuncel H, Tanaka S, Oka S, et al. PARP6, a mono(ADP-ribosyl) transferase and a negative regulator of cell proliferation, is involved in colorectal cancer development. *Int J Oncol.* 2012;41(6):2079–2086.
28. Lin AE, Ebert G, Ow Y, et al. ARIH2 is essential for embryogenesis, and its hematopoietic deficiency causes lethal activation of the immune system. *Nat Immunol.* 2013;14(1):27–33.
29. Shibata Y, Oyama M, Kozuka-Hata H, et al. p47 negatively regulates IKK activation by inducing the lysosomal degradation of polyubiquitinated NEMO. *Nat Commun.* 2012;3:1061.
30. Yang CS, Jividen K, Spencer A, et al. Ubiquitin modification by the E3 Ligase/ADP-ribosyltransferase Dtx3L/Parp9. *Mol Cell.* 2017;66(4):503–516.e5.
31. Verheugd P, Forst AH, Milke L, et al. Regulation of NF-κB signalling by the mono-ADP-ribosyltransferase ARTD10. *Nat Commun.* 2013;4:1683.
32. Bonnal S, Vigevani L, Valcárcel J. The spliceosome as a target of novel antitumour drugs. *Nat Rev Drug Discov.* 2012;11(11):847–859.
33. Sakai T, Sameshima T, Matsufuji M, Kawamura N, Dobashi K, Mizui Y. Pladienolides, new substances from culture of Streptomyces platensis Mer-11107. I. Taxonomy, fermentation, isolation and screening. *J Antibiot (Tokyo).* 2004;57(3):173–179.
34. Muraki M, Ohkawara B, Hosoya T, et al. Manipulation of alternative splicing by a newly developed inhibitor of Clks. *J Biol Chem.* 2004;279(23):24246–24254.
35. Zanotto-Filho A, Braganhol E, Schröder R, et al. NFκB inhibitors induce cell death in glioblastomas. *Biochem Pharmacol.* 2011;81(3):412–424.
36. Perez Y, Menascu S, Cohen I, et al. RSRC1 mutation affects intellect and behaviour through aberrant splicing and transcription, downregulating IGFBP3. *Brain.* 2018;141(4):961–970.
37. Vyas S, Matic I, Uchima L, et al. Family-wide analysis of poly(ADP-ribose) polymerase activity. *Nat Commun.* 2014;5:4426.
38. Sato M, Muguruma N, Nakagawa T, et al. High antitumor activity of pladienolide B and its derivative in gastric cancer. *Cancer Sci.* 2014;105(1):110–116.
39. Taniguchi K, Karin M. NF-κB, inflammation, immunity and cancer: coming of age. *Nat Rev Immunol.* 2018;18(5):309–324.